ISBN: 978-3-95450-262-2 ISSN: 2673-5350 doi: 10.18429/JACoW-IBIC2025-TUPMO41

PRELIMINARY DATA ANALYSIS OF AN IPM PROTOTYPE AT CSNS RCS*

M. A. Rehman[1,2], Y. Guo[1,2], Z. Xu[1,2], X. Nie[1,2], M. Liu[1,2], B. Zhang[1,2], R. Yang[†,1,2]
[1]Institute of High Energy Physics, Beijing, China
[2]China Spallation Neutron Source, Dongguan, China

Abstract

To improve the performance of the China Spallation Neutron Source (CSNS) accelerator complex, a non-invasive beam profile monitor is essential for tuning and operating the CSNS 1.6 GeV Rapid Cycling Synchrotron (RCS). A residual gas Ionization Profile Monitor (IPM) prototype has been constructed to address challenges associated with high-intensity beam profile measurement and to enable real-time monitoring. The RCS IPM prototype was improved through troubleshooting and is now capable to measure the bunch by bunch beam profiles. This paper presents the preliminary analysis of the IPM signals, emphasizing on the temporal resolution and the observations of beam profile during the beam injection.

INTRODUCTION

The China Spallation Neutron Source (CSNS) is one of the major scientific facilities in China, constructed to deliver intense pulsed neutron beams for diverse scientific research and industrial applications [1, 2]. Its accelerator complex consists of an 80 MeV linac, a 1.6 GeV rapid cycling synchrotron, a beam transport line, and a solid tungsten target station. Through a multi-turn charge exchange injection process, the 80 MeV H^- beam from the linac is converted into proton and injected in the RCS. Subsequently, the RCS accelerates the proton beam to 1.6 GeV with a beam intensity of 1.56×10^{13} ppb, delivering a beam power of 100 kW to the neutron target. The CSNS power upgrade project (CSNS-II) has been launched aiming to increase the beam power to 500 kW [3]. The major upgrade of the accelerator complex includes the superconducting accelerator downstream of the DTL section, the update of the injection area, and the implementation of the dual-harmonic RF cavities. The primary parameters of both CSNS and CSNS-II are summarized in Table 1. The beam transverse profile information is of great importance for the successful commissioning and operation of a circular accelerator at intensity frontier, such as CSNS RCS. A prototype IPM has been designed and installed in the RCS. This paper presents the preliminary analysis of the IPM signals to extract the temporal resolution and beam profile under the ion-collection mode.

IONIZATION PROFILE MONITOR

The IPM was first proposed and developed in the 1960s [4, 5]. However, due to the complexity of the instrument, experience and debugging are required to ensure its effective operation and accurate results.The IPM system of the CSNS Rapid Cycling Synchrotron (RCS) comprises two primary components: the IPM detector, located in the beam tunnel, and the signal readout system [6]. The IPM field cage consists of 28 electrodes with an aperture of 220 mm × 231 mm, as shown in Fig. 1. To enhance electric field uniformity, adjacent electrodes are interconnected via 100 MΩ resistors. The collection electrodes are gold-coated to suppress secondary electron emission from their surfaces. Additionally, a grounded top electrode features a central rectangular opening of 30 mm × 80 mm, allowing secondary ions and electrons, generated from beam-residual gas interactions, to pass to the Micro Channel Plate (MCP). Following chamber venting and installation, high-voltage conditioning was performed to mitigate potential arcing during IPM operation.

Table 1: CSNS and CSNS–II RCS Parameters

Parameters	CSNS	CSNS–II	Units
Beam Power	100	500	kW
Injection Energy	80	300	MeV
Ring Circumference	227.92	227.92	m
Extraction Energy	1.6	1.6	GeV
Repetition Rate	25	25	Hz
f_{RF}	1.02-2.44	1.02-2.44	MHz
Number of Bunches	2	2	
Beam Intensity	1.56×10^{13}	7.8×10^{13}	ppb

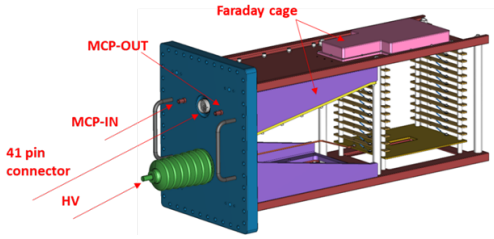

Figure 1: The schematic of the IPM prototype at the CSNS RCS.

A maximum bias voltage of 30 kV has been applied to the field cage after iterative conditioning. To suppress beam-induced electromagnetic interference (EMI), a honeycomb-shaped RF shield is mounted on the center opening, forming a Faraday cage together with the frame and top cover. The honeycomb structure features a hexagonal shape with a width of 3.2 mm and a depth of 6 mm. On the opposite side, an ion trap structure is incorporated to suppress secondary electrons during electron-mode operation. For detecting the

* Work supported by National Natural Science Foundation of China (No. 12305166) and the Natural Science Foundation of Guangdong Province, China (No. 2024A1515010016)
† yangrenjun@ihep.ac.cn

ISBN: 978-3-95450-262-2 ISSN: 2673-5350 doi: 10.18429/JACoW-IBIC2025-TUPMO41

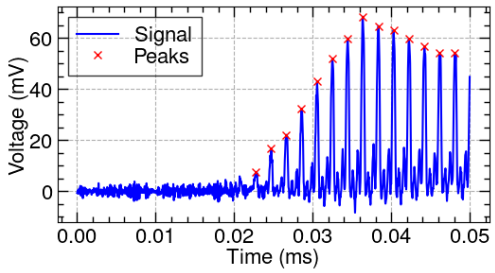

Figure 2: The integrated signal of the 32 anode strips of the IPM's MCP for the 0–0.05 ms time interval.

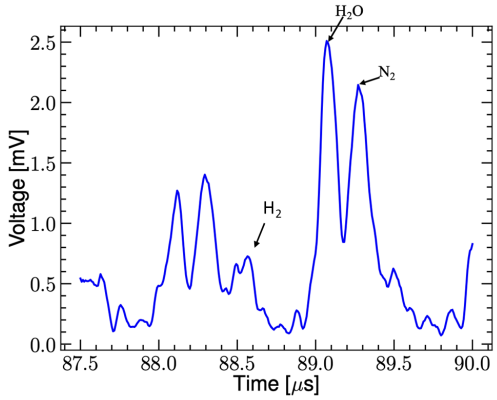

Figure 3: Determination of the primary residual gas components.

collected ions or electrons, a two-stage MCP is employed. The MCP consists of 32 parallel anode strips with a pitch width of 2.5 mm and an effective dimension of 81×31 mm^2. A detailed description of the instrument has been reported in Ref. [6].

DATA ANALYSIS

A typical bunch-by-bunch signal from the IPM is illustrated in Fig. 2. The signal shows the 32-channel summed data. To detect every bunch the peak values of the summed signal are used for subsequent data processing.

The biased voltage at the electrode plate is 25 kV forming a vertical E-field strength of about 110 kV/m. Since the initial velocity of the positive ions is almost at the thermal velocity, the time of flight of ions at the MCP could be approximated as

$$t = \frac{d}{\sqrt{2qV/m}}, \tag{1}$$

where q denotes the ion charge, m is the ion mass, d represents the distance from the center of the field cage to the collector plate, and V is the voltage applied to the field cage. With different masses and arrival time, distinct and separable peaks from different gas species are observed. According to the time of flight ratio between the three dominant peaks, the primary gas components can be inferred as H_2, H_2O, and N_2. The signal from H_2^+, H_2O^+, and N_2^+ ions is shown in Fig. 3.

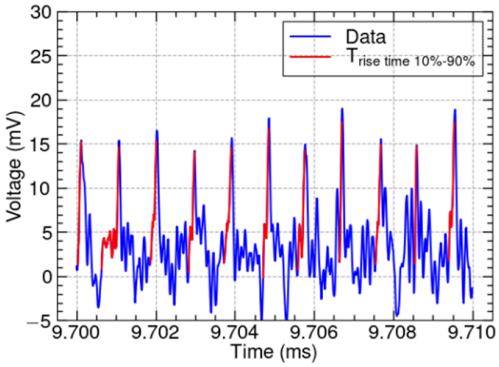

Figure 4: Determination of IPM temporal resolution.

In comparison to the ion collection time (~ μs), the electron collection time is approximately 10–20 ns, depending on the electric field strength of the field cage. The root-mean-square (rms) bunch length of the beam is approximately 120 ns at injection and is then compressed to about 20 ns at beam extraction. Therefore, the IPM signal in electron-mode before beam extraction is used to assess the temporal resolution of the IPM.

The temporal resolution, determines the detector's response capability to rapid signal variations, while the bandwidth directly limits the ability to resolve short-duration events in particle beams. A superior temporal resolution enables the capture of higher-frequency signal components, while a lower resolution results in signal deterioration and loss of fine details. The relationship between the temporal resolution Δt and the system bandwidth Δf (typically the 3-dB bandwidth) is approximated by

$$\Delta t \approx 0.35/\Delta f, \tag{2}$$

where Δf is the -3 dB system bandwidth, Δt represents the rise time from 10 % to 90 % of the signal amplitude. Through calculations tailored to this IPM, it is determined that a system bandwidth greater than 3.5 MHz yields a temporal resolution approaching 100 ns, sufficient for resolving the injection bunch length. The rise time of the dominant peaks in electron mode is shown Fig. 4.

Beam Profiles in Ions Collection Mode

A peak-finding algorithm was developed to accurately identify individual electron bunches on a bunch-by-bunch basis, enabling the construction of a horizontal beam profile using peak values from all 32 channels of the MCP detector. To ensure precise detection of bunch peaks, the parameters of the peak-finding function were optimized. The experiment was performed in single bunch injection mode. By extracting the signal amplitude (sum signal) from each channel at the detected peaks, the bunch-by-bunch beam profile was reconstructed. The horizontal beam profiles for the first 100 turns are presented in Fig. 5.

The 2D density map of the horizontal beam profile for the first 1 ms is illustrated in Fig. 6. It can be observed that the signal amplitudes are significantly reduced beyond 0.2 ms

ISBN: 978-3-95450-262-2 ISSN: 2673-5350 doi: 10.18429/JACoW-IBIC2025-TUPMO41

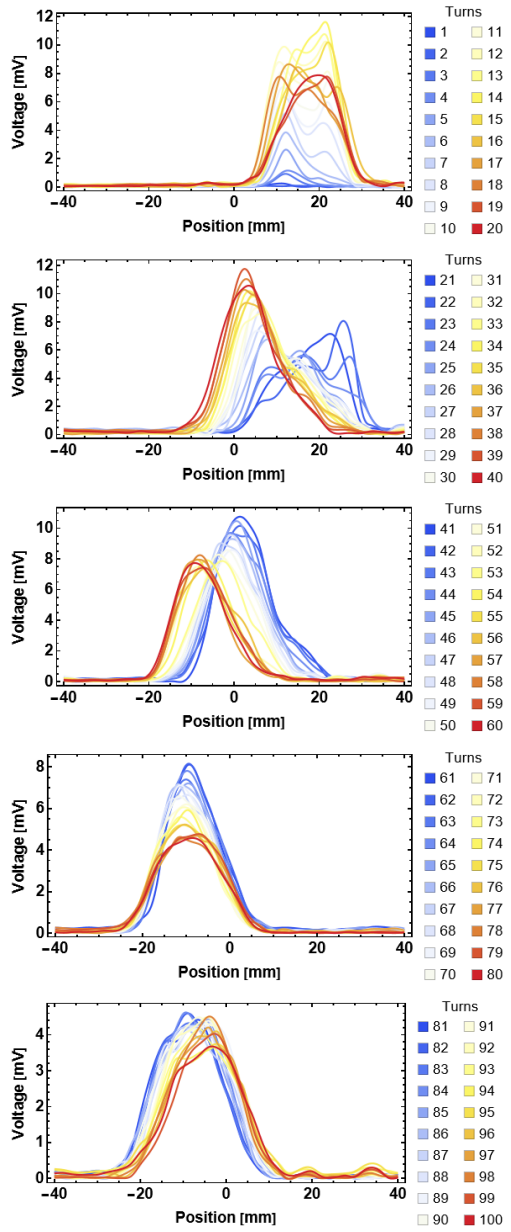

Figure 5: The observed horizontal beam profiles of the first 100 turns.

due to MCP saturation [7]. To address the MCP saturation issue, a gated field cage [8] is currently under design.

After obtaining the one-dimensional beam profiles, the temporal evolution of the transverse beam center and the RMS beam size can be further computed. The beam center (μ_x) can be calculated using the intensity-weighted average

$$\mu_x = \frac{\sum x_i I_i}{\sum I_i}, \tag{3}$$

and the RMS beam size (σ_x) is given by

$$\sigma_x = \sqrt{\frac{\sum I_i (x_i - \mu_x)^2}{\sum I_i - 1}}, \tag{4}$$

where I_i represents the intensity of the signal at position x_i.

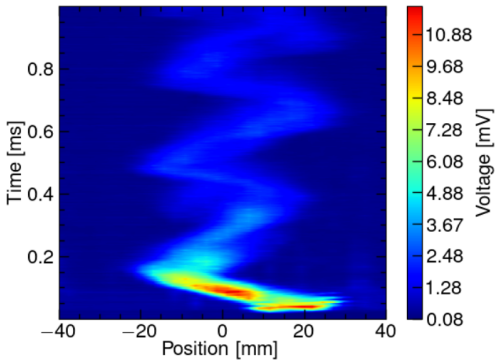

Figure 6: The horizontal bunch-by-bunch beam profile over 0-1 ms for an injected H^- pulse width of 85 μs.

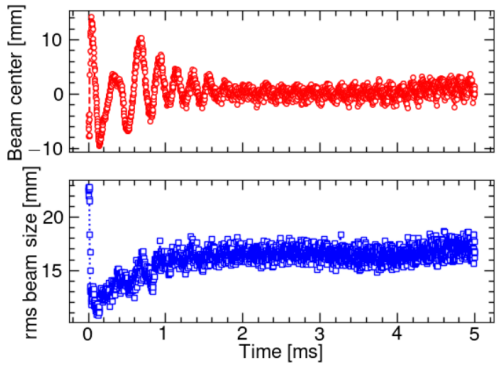

Figure 7: The evolution of the beam rms horizontal beam profile and center for the first 0-0.5 ms.

Given a linac pulse width of 85 μs and a chopping rate of 90 %, the dipole oscillation of the beam orbit and the beam size have been observed, as shown in Fig. 7. The oscillation of the beam center gradually decreases over time, indicating the occurrence of beam decoherence, while the increase in the rms beam size demonstrates that the beam is smearing out in phase space. The IPM is located in the arc section of RCS, and the horizontal beam profile is dominated by the energy spread and horizontal dispersion. Hence, the oscillation frequencies of the beam center and the rms beam size is coincident with the synchrotron tune.

CONCLUSION

The bunch-by-bunch beam profiles in the CSNS RCS were successfully measured using the IPM. Analysis of the bunched signals in ion collection mode revealed that the residual gas in the RCS beam pipe primarily consists of H_2, H_2O, and N_2. Through detailed signal processing, the temporal evolution of the beam profile in the RCS was successfully reconstructed, enabling the determination of the beam center variation and the RMS beam size. This preliminary result validates the functionality of the IPM system. However, it was observed that the MCP experienced saturation after 0.2 ms, indicating that targeted improvements to the IPM system will be necessary in subsequent work.

ISBN: 978-3-95450-262-2 ISSN: 2673-5350 doi: 10.18429/JACoW-IBIC2025-TUPMO41

REFERENCES

[1] H. Chen *et al.*, "Design and construction of the China Spallation Neutron Source", *Nucl. Instrum. Methods Phys. Res. A*, vol. 1078, p. 170431, 2025. doi:10.1016/j.nima.2025.170431

[2] W. Sheng *et al.*, "Introduction to the overall physics design of CSNS accelerators", *Chin. Phys. C*, vol. 33, no. S2, p. 1, 2009. doi:10.1088/1674-1137/33/S2/001

[3] H. Liu and S. Wang, "Longitudinal beam dynamic design of 500 kW beam power upgrade for CSNS-II RCS", *Radiat. Detect. Technol. Methods*, vol. 6, no. 3, pp. 339–348, 2022. doi:10.1007/s41605-022-00325-5

[4] V. Dudnikov, "The intense proton beam accumulation in storage ring by charge-exchange injection method", Ph.D. thesis, Novosibirsk INP, Novosibirsk, Russia, 1966.

[5] J. Fred Hornstra and W. H. DeLuca, "Nondestructive Beam Profile Detection Systems For The Zero Gradient Synchrotron", in *6th International Conference on High-Energy Accelerators*, Cambridge, Massachusetts, Sep. 1967, pp. 374–377.

[6] M. Rehman *et al.*, "Troubleshooting the ionization profile monitor (IPM) for CSNS 1.6 GeV RCS", in *Proc. IBIC'24*, Beijing, China, Sep. 2024, pp. 301–304. doi:10.18429/JACoW-IBIC2024-WEP18

[7] T. Kawakubo, T. Ishida, E. Kadokura, Y. Ajima, and T. Adachi, "Fast data acquisition system of a non-destructive profile monitor for a synchrotron beam by using a microchannel plate with multi-anodes", *Nucl. Instrum. Methods Phys. Res. A*, vol. 302, no. 3, pp. 397–405, 1991. doi:10.1016/0168-9002(91)90352-Q

[8] K. Satou, S. Igarashi, and Y. Sato, "Merits of pulse mode operation of residual gas ionization profile monitor for J-PARC main ring", in *Proc. IBIC'22*, Kraków, Poland, Sep. 2022, pp. 434–437. doi:10.18429/JACoW-IBIC2022-WEP21